If we take into account scattering of the electrons by phonons as well as by impurities, we have

$$\langle 1/\tau\rangle=\langle 1/\tau\rangle_{\text{phonon}}+\langle 1/\tau\rangle_{\text{impurity}}. \quad \text{(A14)}$$

For spherical energy surfaces and acoustic anisotropy, Holstein[12] has obtained an expression for $\langle 1/\tau\rangle_{\text{phonon}}$, viz.

$$\langle 1/\tau\rangle_{\text{phonon}}=\frac{2}{5}\frac{\theta}{T}\frac{1}{\tau}. \quad \text{(A15)}$$

In any case, we can use (A13) and (A11) to write the total absorptivity in the form

$$A=A_{\text{surface}}+A_{\text{volume}}+\left(\frac{m}{\pi Ne^2}\right)^{\frac{1}{2}}\langle 1/\tau\rangle, \quad \text{(A16)}$$

where $\langle 1/\tau\rangle$ is now understood to refer to the *impurity* relaxation time.

[12] T. Holstein, Phys. Rev. **96**, 535 (1954).

Now the impurity resistance ρ_{impurity} is given by the equation

$$\rho_{\text{impurity}}=m/Ne^2\langle\tau\rangle, \quad \text{(A17)}$$

where

$$\langle\tau\rangle=\int\tau v dS\Big/\int v dS. \quad \text{(A18)}$$

Using these equations, (A15) may be written in the form

$$A=A_{\text{surface}}+A_{\text{volume}}+\langle\tau\rangle\langle 1/\tau\rangle(Ne^2/\pi m)^{\frac{1}{2}}\rho_{\text{impurity}}, \quad \text{(A19)}$$

which is the same equation as derived previously. From the Schwarz inequality, it may be shown that

$$\langle\tau\rangle\langle 1/\tau\rangle\geq 1, \quad \text{(A20)}$$

the equality only holding for *isotropic* impurity scattering.

PHYSICAL REVIEW VOLUME 121, NUMBER 2 JANUARY 15, 1961

Electron Scattering by Thin Foils for Energies Below 10 kev

H. KANTER
Electronics and Nuclear Physics Department, Westinghouse Research Laboratories, Pittsburgh, Pennsylvania
(Received May 23, 1960; revised manuscript received September 19, 1960)

The transmission (η_T) of electrons through thin films of C, Al_2O_3, Al, Ni, Ag, and Au, together with their distribution in angle and energy, were measured in a spherical retarding-potential analyzer. The distributions were characterized by average and most probable scattering angle, average and most probable fractional energy loss, etc. The dependence of these variables on initial energy (E_p), film thickness, and material was investigated. For sufficient film thickness, the transmitted energies, the scattering angles and η_T can be represented as universal functions of the reduced energy, E_p/E_c, where E_c is the critical E_p for the onset of transmission. Direct relations exist between η_T, scattering angles, and energy losses for the complete range of scattering from small-angle scattering to total diffusion. The dependence of η_T and average fractional energy loss on Z is consistent with published results on backscattering coefficient and energy loss for thick layers. An estimate of the mean free path for inelastic collisions proves to be in good agreement with the predictions of the Bohr-Bethe theory. Range-energy relations are almost independent of Z when the range is measured in mass per unit area.

INTRODUCTION

UPON passing through relatively thick layers of solid matter, electrons generally undergo a considerable number of collision processes in which they gradually lose their energy and change their direction. Although the individual collision processes are rather well understood in terms of elastic nuclear scattering, inelastic scattering on atomic electrons and collisions with the conduction electron plasma, a complete theoretical description of the plural and multiple scattering process, including elastic and inelastic collisions, is at present not possible.[1] Only for certain limiting cases does a successful theoretical treatment of the multiple scattering process exist. Molière[2] described multiple scattering for small individual deflections, not including any energy loss. The diffusion of high-energy electrons as a result of elastic collisions was treated by Bothe,[3] Bethe, Rose, and Smith[4] and more recently by Molière.[5] The energy-loss distribution of electrons passing through solids due to inelastic scattering without appreciable deflection has been calculated by Landau, Blunk, and Leisegang, and others.[6] The average rate of energy loss of electrons along their path is well described by Bethe's stopping

[1] See for instance: R. D. Birkhoff, *Handbuch der Physik* (Springer-Verlag, Berlin, 1958), Vol. 34, p. 53.
[2] G. Molière, Z. Naturforsch **3a**, 78 (1948).
[3] W. Bothe, Z. Physik **54**, 161 (1928).
[4] H. A. Bethe, M. E. Rose, and L. P. Smith, Proc. Am. Phil. Soc. **78**, 573 (1938).
[5] G. Molière, Z. Physik **156**, 318 (1959).
[6] L. Landau, J. Phys. U.S.S.R. **8**, 201 (1944); I. Blunck and S. Leisegang, Ann. Phys. **128**, 500 (1950); K. C. Hines, Phys. Rev. **97**, 1725 (1955); R. M. Sternheimer, Phys. Rev. **103**, 511 (1956).

power formula,[7] although the mean excitation potential of the scattering material must generally be determined empirically.[8] More recently, Spencer[9] calculated the energy dissipation of electrons in solids for incident energies above 50 kev.

However, for electron energies below 10 kev the existing theories of multiple scattering do not apply, since, contrary to the assumptions made in the various theories, a single inelastic collision can lead to a relatively large deflection and a relatively high-energy loss. Furthermore, the cross section for inelastic collisions in this energy range depends critically on the intial energy of the incoming electrons because of the changing participation of inner-shell electrons in the scattering process. Therefore, experimental investigations in this energy range are of interest, since they can serve to guide the development of a theory applicable at low energies.

A number of measurements at energies below 10 kev have involved a study of the backscattered electrons from solids. The variation of the backscattering coefficient with initial electron energy[10–12] has been studied, as well as its dependence on angle of incidence.[13] Other studies in this energy range include characteristic energy losses[14] and energy straggling distributions.[11,13]

Measurements on the transmission of electrons in the energy range below 10 kev were to a large part designed to test existing range-energy relations.[15,16] The energy distribution of electrons transmitted through thin foils of various materials were reported by Ruthemann and Lang[17] at a few kev. However, these authors were primarily interested in the fine structure due to characteristic energy losses and accompanying small angular deflections.[18] Only Young[19] reported complete energy spectra obtained for electrons that passed through Al_2O_3 films in this energy range. No detailed studies on both the energy and angular distributions covering the whole range of transmitted energies and deflection angles for the exit side of thin foils have been reported in the literature.

In recent years the techniques for the preparation of very thin, freely supported films of various materials have been greatly improved. This opened the possibility of extending transmission measurements to lower energies than previously accessible. The objective of the work reported below is to describe the plural and multiple scattering process at low energies as completely as possible in its dependence on important parameters such as initial energy, film thickness, and material. Thereby emphasis is placed on the over-all characteristics of the scattered electrons, such as the fraction of electrons transmitted by a foil, the average and most probable angular deflection and the average and most probable energy loss. Any "fine structure" in the angular or energy distributions due to coherent scattering or characteristic energy losses are disregarded. These effects are better observable at higher energies where the collision mean free path is greater since the large number of individual collisions undergone by a low-energy electron tends to wash out all fine structure. Information of the type reported here is not only desirable for a more complete understanding of such processes as secondary electron emission, bombardment-induced conductivity, and cathodoluminescence, but it is also of direct interest in various physical and radiological applications involving the penetration of low-energy electrons into solids.

APPARATUS AND EXPERIMENTAL TECHNIQUES

For the purpose of measuring angular and energy distributions, a simple retarding technique employing a spherical collector was used as shown in Fig. 1. In order to measure angular distributions the collector was divided into concentric zones. The limit in angular resolution of a few degrees which can be obtained in such an arrangement seemed to be sufficient, since only the over-all scattering behavior was to be investigated, disregarding any fine structure. Such an arrangement has the advantage that a large fraction of the scattered electrons contribute to the zonal collector currents, thus allowing relatively simple means for detection.

Thin film targets were mounted on small tubes which could be easily inserted into electrode T. The target was positioned in the center of the spherical grids G_1

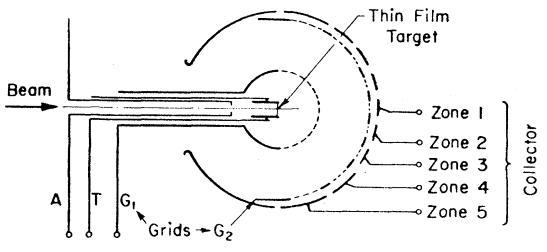

FIG. 1. Schematic of electron analyzer.

[7] H. A. Bethe, Ann. Physik **5**, 325 (1930).
[8] For a review on stopping power see W. Brandt, Health Phys. **1**, 11 (1958).
[9] L. V. Spencer, Phys. Rev. **98**, 1957 (1955).
[10] P. Palluel, Compt. rend. **224**, 1492 (1947); T. L. Matskevitch, J. Tech. Phys. U.S.S.R. **27**, 289 (1957) [translation: Soviet Phys.—Tech. Phys. **2**, 255 (1957)].
[11] E. J. Sternglass, Phys. Rev. **95**, 345 (1954).
[12] J. E. Holliday and E. J. Sternglass, J. Appl. Phys. **28**, 1189 (1957).
[13] H. Kanter, Ann. Physik **20**, 144 (1957).
[14] E. Rudberg, Proc. Roy. Soc. (London) **A127**, 111 (1933) and Phys. Rev. **50**, 138 (1936); R. P. Reichertz and H. E. Farnsworth, Phys. Rev. **75**, 1902 (1949); C. J. Powell and J. B. Swan, Phys. Rev. **115**, 869 (1959).
[15] C. Feldman, Phys. Rev. **117**, 455 (1960); for a review on earlier range data see Y. P. Varshni and R. C. Karnatak, Ann. Physik **2**, 413 (1959).
[16] J. R. Young, J. Appl. Phys. **27**, 1 (1956) and Phys. Rev. **103**, 292 (1956).
[17] G. Ruthemann, Ann. Physik **2**, 113 (1948); W. Lang, Optic **3**, 233 (1948).
[18] For a review on characteristic energy losses see L. Marton, Revs. Modern Phys. **28**, 172 (1956); D. Pines, Revs. Modern Phys. **28**, 184 (1956).
[19] J. R. Young, J. Appl. Phys. **28**, 524 (1957).

and G_2, which were made of tungsten mesh with four meshes per mm and 0.02-mm wire diameter. The supporting structure of the grids was made of ring-shaped strips which separated the zonal angular ranges. The electron current passing through the grids was collected by five zonal collector electrodes. The grid-supporting strips provided a blind angular range of at least 3° between each zone, covering the openings between the collector electrodes.

A conventional electron gun supplied an electron beam of the order of 10^{-7} amp with a diameter of about 1 mm. The beam was centered with the help of aperture A (diameter 3 mm). The aperture was held at a negative potential with respect to the target to suppress slow secondary electrons emitted from the back side of the target. The impinging current was measured at the target by connecting it to all the surrounding electrodes of the analyzer. The error due to backscattered electrons from the target escaping into the solid angle subtended by the aperture could be neglected.

In order to determine the fraction of electrons transmitted by a foil the electron current leaving the foil was measured with grid G_1 as collector. This grid was tied electrically to both G_2 and the collector electrodes and was held at a potential of 45 v negative with respect to the target, thus repelling secondary electrons with energies smaller than 45 ev emitted by the target. Grid G_1, like all other electrodes of the analyzer, was covered with soot in order to reduce backscattering and secondary electron emission. The transmission current was corrected for the small secondary electron current flowing back from grid G_1 to the target. This current was between 6 and 10% of the collected current, depending on the initial electron energy.

In order to measure the angular and energy distribution of the transmitted electrons, grid G_1 was tied electrically to the target. An opposing potential was applied between grid G_1 and G_2. The collector current of each zone was measured as a function of this opposing potential.

Grid G_1 was necessary to keep the space in front of the target field-free, and thus to avoid defocusing of the emerging electrons. Without grid G_1, nonradial field components in front of the target were found to give rise to considerable errors in the measured angular and energy distributions.[20] The lens effect introduced by the mesh was calculated with a formula similar to that used by Jonker.[21] The angular deviation of an electron passing through the grid was smaller than 1.5° and the corresponding decrease in energy resolution of the analyzer was about 0.8 ev, in agreement with measurements.

The collector was held at a potential of 45 v positive with respect to grid G_1, which served to suppress secondaries emitted by the collector electrodes. Only backscattered electrons with energies greater than 45 v were therefore able to leave the collector. The backscatter coefficient for carbon is about 6% and is practically constant with the energy of the impinging electrons.[10,11] As a result, changing the retarding potential and thereby altering the average energy of the electrons impinging at the collector did not introduce significant error in determining the true shape of the integral energy spectrum.

The over-all energy resolution of the analyzer was about 3 ev. This was estimated from the linewidth of elastically scattered electrons in the differential energy spectrum. The differential energy spectrum was measured by adding an ac voltage to the retarding potential and measuring the ac component of the collector current in a method quite similar to that described by Leder and Simpson.[22] Since this method is not used in the measurements described here, a detailed description will be given elsewhere. For sufficiently thin foils the peaks due to the principal characteristic energy losses were readily observable.

Angular distributions were generally plotted as the relative number of electrons deflected into the unit interval of scattering angle θ as a function of θ, integrated over the azimuth. In order to obtain this quantity from the data, the measured zonal collector currents had to be divided by the corresponding angular ranges. The geometrical angular ranges of the zones were determined with an accuracy of better than $\frac{1}{2}$°. Zone 1 extended from 0° to 3.6°, zone 2 from 6.9° to 11.3°, zone 3 from 14.3° to 18.5°, zone 4 from 25° to 42.5°, and zone 5 from 49.8° to 82.4°. The lens effect of grid G_1 mentioned above, however, tends to decrease somewhat the actual angular ranges. Because variations of the open areas of grids G_1 and G_2 can introduce relative errors into the zonal collector currents, the open area of these grids was determined by measuring the transmission of light through both grids from a small source placed in the center of the analyzer. The transmission varied from 55% to 62%, introducing a relative error in the zonal collector currents of ±6%.

For electron energies larger than 5 kev and very thin films (≤ 10 $\mu g/cm^2$), inelastic scattering on grid G_1 caused an anomalous increase of the zonal collector currents at low retarding potentials (see Fig. 6). Such an effect was also observed without any foil in the analyzer. Any such anomalous increases were therefore disregarded. Because the retarding potential curves usually had a nearly constant slope over almost half the total energy range, the curves were extrapolated with a constant slope up to zero potential. The deviations were never larger than 15% of the collector current and the remaining uncertainty is believed not to have increased the error in the relative zone currents to a total of more than ±8%.

The analyzer was mounted in a magnetically shielded,

[20] N. A. Soboleva, Radiotekh. i Elektron. **3**, 339 (1958).
[21] J. L. H. Jonker, Philips Research Repts. **6**, 372 (1941).
[22] L. B. Leder and J. A. Simpson, Rev. Sci. Instr. **29**, 571 (1958).

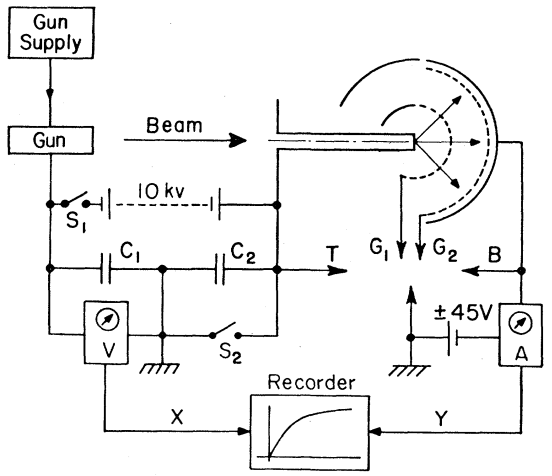

FIG. 2. Block diagram of apparatus.

bakeable vacuum system. After a foil was inserted in the analyzer, the system was baked for about 12 hr at 250°C to 300°C. With the filament of the electron gun in operation, the pressure was generally in the order of 10^{-7} mm Hg. No appreciable formation of carbonaceous layers on the target surface due to the presence of pump-oil vapors was observed during operation. This could be concluded from the fact that the secondary electron yield of a given target, which is known to depend sensitively on the amount of carbon on the surface, did not change in the course of several hours of bombardment. The measurements on a given foil were usually completed within two hours.

A block diagram of the circuit used is shown in Fig. 2. The electron gun, the gun supply, the target (together with aperture A of Fig. 1), and the batteries supplying the beam voltage were all isolated from ground. In order to determine the fraction of electrons that have passed through the foil, grids G_1 and G_2 were connected with the collector B. The switches S_1 and S_2 were closed. Thus the target was at ground potential, while the grids and the collector were held at a potential of 45 v negative with respect to the target. The beam energy was changed by opening switch S_1. Condenser C_1 was discharged through the voltmeter resistance, thus gradually decreasing the beam voltage to the point where no electrons were able to pass through the foil. An x-y recorder, driven by the meters V and A, plotted the collector current directly as a function of the beam energy.

In order to plot the collector current as a function of the retarding potential, grid G_1 was connected to the target T and grid G_2 was grounded. The collector had a potential of +45 v with respect to ground. Switch S_1 remained closed. With S_2 closed the retarding potential between grids G_1 and G_2 was zero. Upon opening S_2 the condensers C_1 and C_2 were recharged through the voltmeter resistance, thus gradually increasing the target potential to the point where no electrons were able to pass through grid G_2 to reach the collector. The recorder plotted directly the integral energy spectrum.

TARGET PREPARATION

For the range of electron energies and foil thicknesses considered here, the surface condition of the film targets is of relatively small influence. Therefore the film preparation technique described below, which does not provide samples free from absorbed gases and oxide, appeared to be adequate.

All metal films were prepared by rapid vacuum evaporation onto a supporting nitro-cellulose film, stretched across the end of a tube of 6-mm inside and 8-mm outside diameter. The supporting film was removed by baking in air at about 200°C for one hour.[23] Each film was checked for pinholes under the microscope. Any tears or holes occurring in the film during the experiment could be easily found in transmission measurements, since in the presence of holes the transmitted current would not drop completely to zero upon decrease of the initial electron energy. During the preparation of the film, the metal was simultaneously evaporated onto glass slides which (after a subsequent silver evaporation) were used to determine the thickness by multiple beam interferometry.[24] The thickness measurements by this technique are believed to be accurate to within ±5% or ±25 A, whichever is the larger. Using the density of bulk material the film thickness was converted to mass per unit area.

The foil thickness determined in this fashion can be expected to represent the actual film thickness only if no oxidation or oxygen uptake changes the mass density of the film during the bake-out procedure. Furthermore, it must also be assumed that the accommodation coefficient of the glass slides used does not differ greatly from that of the nitro-cellulose film on which the target is prepared, and that the bulk density may be used even for the thinnest films measured. Because it is difficult to be certain of the two latter assumptions, the absolute thickness determinations of the foils are believed to have an accuracy of only about ±10% or ±2 μg, respectively.

In the case of aluminum, where the oxidation is particularly severe, a correction for the presence of an oxide was made as follows. From earlier studies it is known that aluminum films of 150 A thickness can be completely converted to aluminum oxide during bake-out, while 200-A films stay conductive and do not lose their metallic appearance.[25] In order to account for the increases in mass due to oxidation, therefore, each measured film thickness was increased by 3.5 μg/cm^2, which corresponds to the weight of oxygen necessary

[23] M. Garbuny, T. P. Vogl, and J. R. Hansen, Westinghouse Reserach Laboratory Report 71F189-R7-X (unpublished).

[24] See for instance: G. D. Scott, T. A. McLauchlan, and R. S. Sennet, J. Appl. Phys. **21**, 843 (1950).

[25] This is in agreement with measurements of oxidation rates of aluminum by E. A. Gulbransen and W. S. Wyson, J. Phys. & Colloid Chem. **51**, 1087 (1947).

to convert 150 A of Al into Al_2O_3. With this correction, the practical range-energy relations determined for the films (Fig. 5) agreed with the published data by Young[16] to within the experimental error.

According to Gulbransen and Andrew[26] the reaction of nickel surfaces with oxygen for temperatures below 400°C is negligible, so that no corrections were applied for this material. Since surface layers add only very little mass per unit area to foils of heavier material, no corrections of film thicknesses were made for silver and gold films.

Carbon films were prepared by evaporation in vacuum from carbon electrodes heated by high currents.[27] The carbon was deposited on slides covered with a thin layer of KCl, which was subsequently dissolved away in water, allowing the carbon film to be picked up from the surface with the aid of a small wire frame and placed directly on the tubular target holder.

The thickness of the carbon films could not be measured by interferometry since the measurements resulted in very widely scattered data for the range-energy relations, presumably due to wide fluctuations in the density of the films. A similar observation was reported by Agar,[28] who compared interferometric thickness measurements with light transmission data. He found a similarly large scatter in the transmission-thickness relation. To circumvent this difficulty, the thickness of one of the carbon films was determined by quantitative chemical analysis. The resulting range-energy relation agreed very well with the range-energy relation for aluminum and aluminum oxide measured in mass per unit area. The thicknesses of the remaining carbon films could therefore be deduced from the energy corresponding to penetration as defined below, using the known range-energy relation for aluminum.

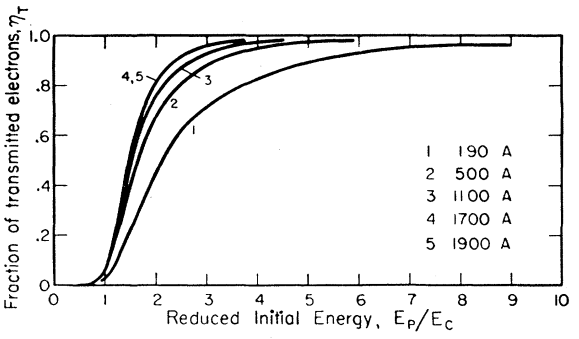

FIG. 3. Fraction of transmitted electrons as a function of reduced initial energy for carbon films of different thickness. No points are shown since the curves were originally plotted by an x-y recorder.

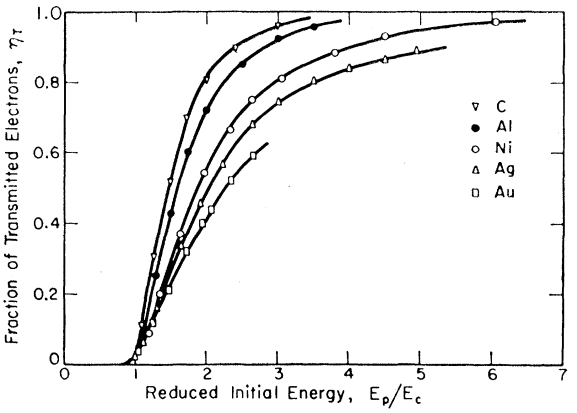

FIG. 4. Fraction of transmitted electrons as a function of reduced initial energy for materials of different atomic numbers with thicknesses ≥ 15 $\mu g/cm^2$.

Aluminum oxide films were prepared by an anodizing technique described in detail in the literature.[29]

RESULTS

1. Transmission of Electrons

The fraction of transmitted electrons, η_T, was measured for each material as a function of the initial energy, E_p, on films of various thicknesses. For the presentation of the transmission curves, a method was used which is believed to have first been suggested by Wecker.[30] By extrapolating to the abscissa the steep part of the transmission curves as a function of E_p, a critical energy for the onset of transmission, E_c, can be defined which is closely related to the film thickness. Transmission curves were then plotted as a function of the reduced energy E_p/E_c, where the initial energy is measured in units of E_c.

Transmission curves plotted in this manner are shown in Fig. 3 for carbon films of various thicknesses. As can be seen, the transmission curves approach a universal transmission curve for carbon in the limit of large film thicknesses. The thickness beyond which the universal curve begins to be valid is of the order of 1000 A or 20 $\mu g/cm^2$. For corresponding curves obtained on aluminum films, the deviation from the universal curve at the smallest thickness of 170 A was about half as large as that for the thinnest carbon film. For the heavier materials, Ni, Ag, and Au, no deviation at all was found at any thickness studied. All these films, however, were thicker than about 15 $\mu g/cm^2$. Thus it is possible to present the transmission properties of a given material by means of a single universal curve applicable for all thicknesses beyond about 20 $\mu g/cm^2$. The universal transmission curves for all the materials investigated are plotted in Fig. 4. The curves obtained

[26] E. A. Gulbransen and K. F. Andrew, J. Electrochem. Soc. **101**, 128 (1954).
[27] E. E. Bradley, J. Appl. Phys. **27**, 1399 (1946); G. Dearnaley, Rev. Sci. Instr. **31**, 187 (1960).
[28] A. W. Agar, Brit. J. Appl. Phys. **8**, 35 (1957). See also: A. Cosslett and V. E. Cosslett, Brit. J. Appl. Phys. **8**, 374 (1957).
[29] W. Walkenhorst, Naturwissenschaften **34**, 373 (1947); G. Hass, J. Opt. Soc. Am. **39**, 532 (1949); L. Harris, J. Opt. Soc. Am. **45**, 27 (1955).
[30] F. Wecker, Ann. Physik **40**, 405 (1941).

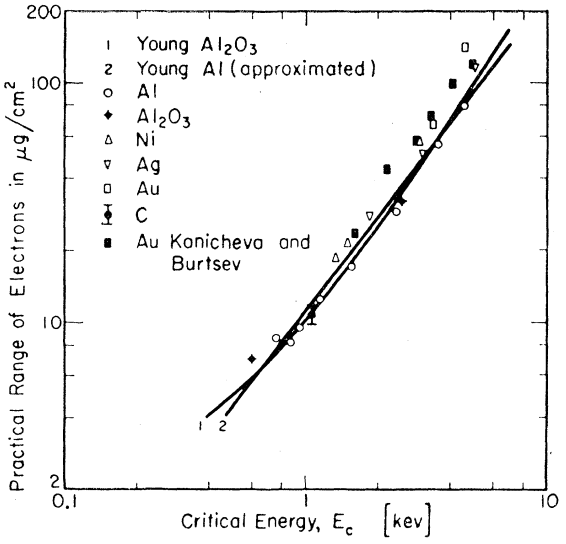

FIG. 5. Practical range-energy relation.

for Al and Au agree very well with those measured by Wecker[30] at initial energies from 20 to 70 kev.

The presentation of data as a function of E_p/E_c rather than separately as functions of E_p and E_c (or film thickness D) turned out to be convenient not only for the transmission but also for the scattering angle and the residual energy of the transmitted electrons. For all these quantities universal presentations were possible. Therefore, once the critical energy E_c for a particular film is known, the scattering behavior for any initial energy can be obtained from the universal curves.

2. Range-Energy Relations

The relation between film thickness and critical energy, E_c, commonly referred to as the practical range-energy relation, is shown in Fig. 5 for all the materials, studied. The range is measured in mass per unit area. Range-energy curves for energies below 10 kev were published by several authors. However, there is no unique definition for the range. Therefore, our data are only compared with those of Young[16] and Kanitcheva and Burtsev,[31] who studied aluminum oxide, aluminum, and gold in the energy range under consideration here, and who defined the range in the same way as in the present work. When the results for aluminum are corrected for the formation of an oxide layer during the film preparation, the data of these authors agree with the present measurements to within the experimental error.

For nickel, silver, and gold, the practical range is found to be slightly higher than for aluminum; but there is insufficient data to establish any systematic trend with the atomic number. The result that the range-energy relation is almost independent of Z for energies below 5 kev agrees with the measurements of Holliday and Sternglass[32] using a backscattering technique. The absence of any strong Z dependence has been explained qualitatively as follows[32]: At energies of a few kilovolts the nuclear screening for high-Z materials is so effective that the penetration depth of the electrons is essentially determined by inelastic scattering processes involving the excitation and ionization of the atomic electrons. Thus the range is approximately inversely proportional to the rate of energy loss, which varies essentially as the number of electrons per atom or the atomic number Z. Since the atomic mass also increases nearly linearly with Z, the range-energy relation should be independent of Z when measured in mass per unit area, as indicated by the data.

3. Energy Distributions

Since in the present study the scattering behavior of electrons as a functions of initial energy, film thickness,

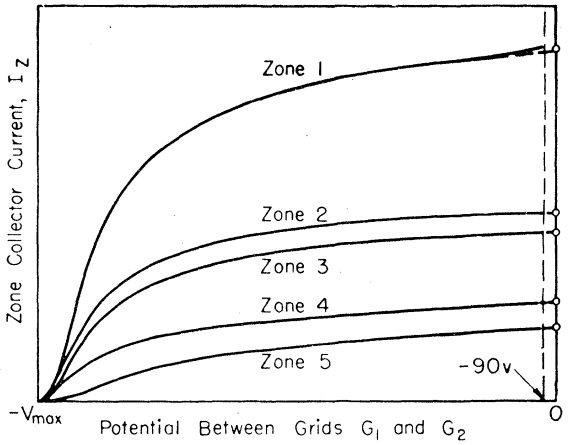

FIG. 6. Typical retarding potential curves (520-A aluminum, $E_p=3900$ ev). Note the increase of the collector current of zone 1 near 0.

and material were investigated for a large number of cases, it is not feasible to reproduce all measured energy and angular distribution curves separately. The distributions were instead characterized by certain quantities which allow one to combine the results in a more general and compact form.

One may characterize the principal features of the energy distribution by two quantities: the average energy E_a and the most probable energy E_w. These quantities were determined by graphical integration and differentiation of the integral energy spectra. The integral spectra were obtained from the zonal collector currents as functions of the retarding potential, applied between grids G_1 and G_2. They were measured for films of different thicknesses and for different initial energies. A typical example is shown in Fig. 6. The straight part

[31] I. R. Kanicheva and V. A. Burtsev, Fiz. Tverdogo Tela. **1**, 1250 (1949).

[32] J. E. Holliday and E. J. Sternglass, J. Appl. Phys. **30**, 1428 (1959).

of the retarding curves, which usually extended from about half the beam potential to less than −90 v, was extrapolated to zero potential. Thus the increase in collector current corresponding to the collection of secondary electrons from the target could be separated out. At the same time, the deviations due to inelastic scattering on grid G_1 mentioned before were excluded by this procedure.

The average and the most probable energy values for electrons scattered into a given zonal angular range were used to calculate the average and most probable energy of all the electrons which have passed through the foil. This was accomplished by an averaging procedure using the solid angles subtended by the collector zones as weight factors. The average fractional energy of all the transmitted electrons, E_a/E_p, as function of the reduced initial energy, E_p/E_c, for carbon films of different thicknesses is shown in Fig. 7. Again a small dependence on film thickness can be observed when plotted in this manner. For the corresponding curves

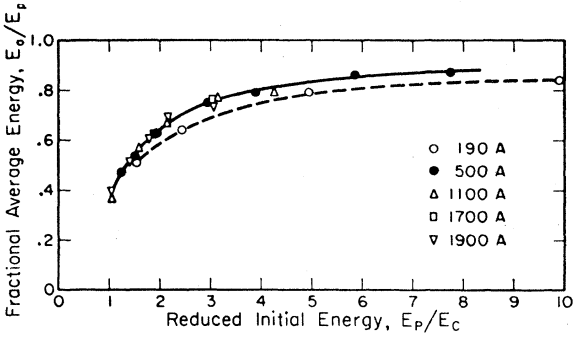

FIG. 7. Fractional average energy as a function of reduced initial energy for carbon films of different thicknesses.

of aluminum, however, no change with film thickness was found to within the experimental accuracy.

The universal curves of the fractional average energy, plotted as a function of E_p/E_c, coincide for all materials investigated as shown in Fig. 8. The consequences of this fact will be discussed below. Figure 9 shows the dependence of the fractional most probable energy, E_w/E_p, as a function of E_p/E_c for various materials.

4. Angular Distributions

The zonal collector currents, obtained by extrapolating the integral energy spectra to zero retarding potential, were used to determine the angular distributions. The angular distributions represent the relative current per unit interval of the scattering angle θ, integrated over the azimuth, as a function of the scattering angle θ. The curves were drawn in such a manner that the ratio of the areas under the curves per zone interval equals the measured ratio of the zonal currents. The angular distributions were characterized by the

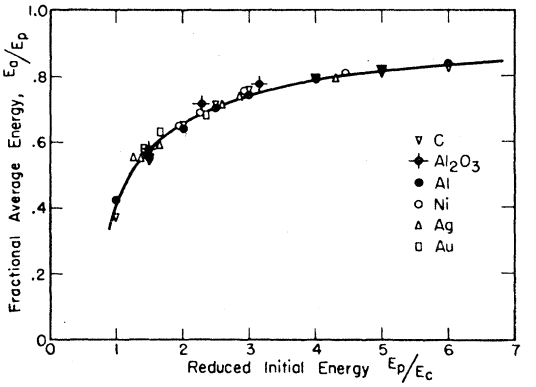

FIG. 8. Fractional average energy of transmitted electrons as a function of reduced initial energy for materials of different atomic numbers with thicknesses ≥ 15 μg/cm^2.

average scattering angle θ_a and by the most probable scattering angle θ_w.[33]

The average scattering angle, θ_a, as a function of E_p/E_c, is independent of the film thickness for all materials investigated. The universal curves of θ_a are shown in Fig. 10. Contrary to the average scattering angle, the most probable scattering angle θ_w observed on C and Al as a function of E_p/E_c (not shown) depends slightly on film thickness. For film thicknesses smaller than 15 μg/cm^2, θ_w is somewhat smaller than the values given by the universal curve. This deviation from the universal curve was observed only for very thin films and low-Z materials such as carbon and to a lesser degree for aluminum. The universal curves of θ_w are shown in Fig. 11.

At very thin foil thicknesses and low Z, deviations from a universal curve therefore occur for the transmission (Fig. 3), the fractional average energy (Fig. 7) and the most probable scattering angle. This fact might

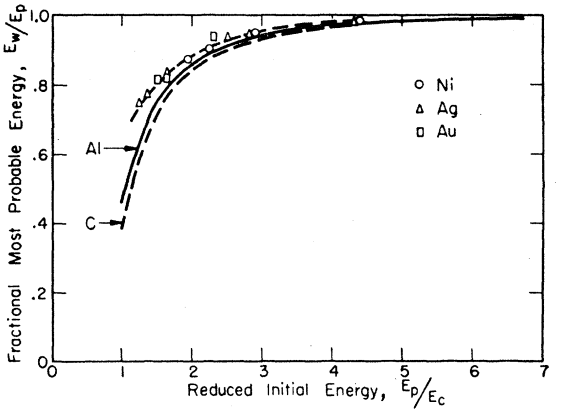

FIG. 9. Fractional most probable energy of transmitted electrons as a function of reduced initial energy for materials of different atomic numbers with thicknesses ≥ 15 μg/cm^2.

[33] Angular distributions of 5–30-kev electrons having traversed thin films of aluminum, covered with MgO, have been reported by B. G. Butkevich and M. M. Butslov, Radiotekh. i Elektron. 3, 355 (1958).

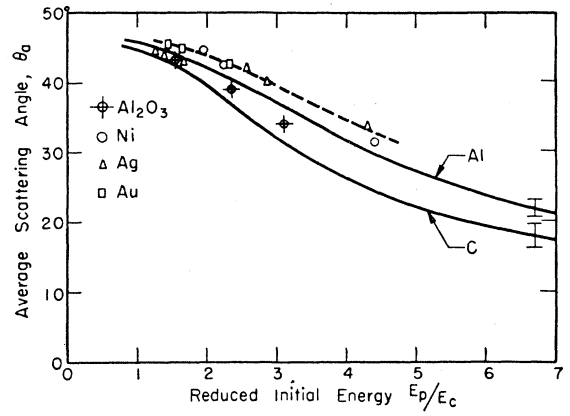

FIG. 10. Average scattering angle as a function of reduced initial energy for materials of different atomic number with thicknesses $\geq 15\ \mu g/cm^2$.

be explained by the preponderance of plural scattering under these conditions, in contrast to multiple scattering for the thicker foils. It should be recalled that E_c is defined in terms of the onset of transmission. When scattering results from only a few small-angle collisions, transmission sets in relatively earlier than when the electrons are strongly scattered. Therefore, curves plotted on an E_p/E_c scale for very thin films of low-Z material are displaced to larger E_p/E_c values with respect to the universal curves valid for the thicker films, as can be seen in Figs. 3 and 7.

The possibility of presenting the scattering data in the form of universal curves as a function of E_p/E_c is not only of practical value but it also allows one to draw certain physical conclusions as will be discussed in the next section.

DISCUSSION

The following discussion is restricted to results obtained for films sufficiently thick so that the data can be represented by universal curves. Since the universal functions all depend on E_p/E_c, direct correlations exist between transmission, scattering angle, and fractional energy loss as will be discussed in detail below.

1. Transmission and Scattering Angle

The variation of the curves for transmission and scattering angles with Z suggests a close relation between transmission and scattering angle. In fact, a plot of transmission as a function of the most probable scattering angle θ_w (Fig. 12) shows that to within the experimental accuracy, this relation is independent of Z as long as the transmission is smaller than 0.6.[34] For $\theta_w \sim 10°$, the difference between the fraction transmitted for carbon and silver is about 10%. Because the relation between transmission and scattering angle appears not to be appreciably affected by materials of various stopping powers, one is led to conclude that the transmission of electrons through thin films depends predominantly on scattering. The influence of actual stopping in the foil can only be a second order effect. The transmission η_T can therefore be used to measure the "scattering power" of a material.

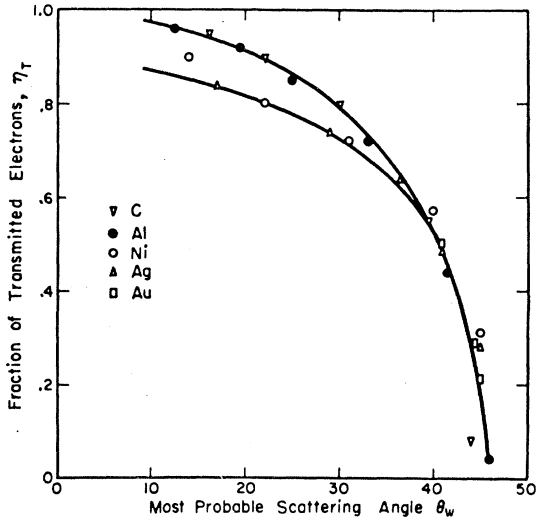

FIG. 12. Fraction of transmitted electrons as a function of the most probable scattering angle for materials of different atomic numbers.

This conclusion is consistent with results by Sternglass,[11] who pointed out that the backscattering coefficient η_B for electrons backscattered from metals is related to the scattering power of the metal. The close correlation between η_B and η_T is shown in Fig. 13, where both quantities are plotted as functions of Z for a film of thickness equal to half the range of the electrons. As shown by Holliday and Sternglass,[12] the number of electrons backscattered from a film of this thickness

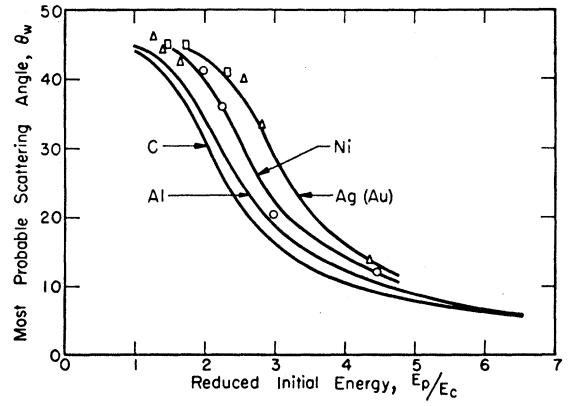

FIG. 11. Most probable scattering angle as a function of reduced initial energy for materials of different atomic number with thicknesses $\geq 15\ \mu g/cm^2$.

[34] Comparison with the most probable scattering angle was made since this angle varies over a relatively wide range. The relation between transmission and the average scattering angle is, however, very similar.

will not increase with further increase of thickness so that the backscattering coefficients for the bulk material apply. The transmitted electrons, however, have traveled only through about half their range, which means that the primary energy is roughly twice as large as the critical energy E_c of this film. Comparison is therefore made with transmission values for $E_p/E_c=2$. Upon adding the transmitted and backscattered fraction of electrons, it is seen that for any film material of thickness corresponding to half the electron range, only 10 to 20% of all electrons are actually stopped in the foil.

The correlation between transmission and the mean squared scattering angle was predicted for "total diffusion" by elementary diffusion theory.[3] Total diffusion is defined as that stage in the scattering process, where no change in the angular distribution at the exit side of the film occurs upon further increase of film thickness. The angular distribution for total diffusion can be approximated by a cosine distribution with $\theta_a=45°$. Referring to Fig. 10, this value of the average

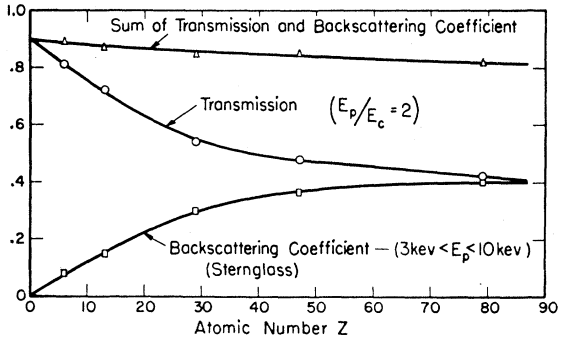

FIG. 13. Relation between transmission and backscattering coefficient of materials as a function of atomic number.

scattering angle is reached for $E_p/E_c\simeq 1$. The physical meaning of the critical energy E_c of a film is therefore the initial energy E_p below which the electrons at the exit side emerge in a state of total diffusion. For $E_p\leq E_c$, Bothe showed that a direct relation exists between a "scattering coefficient" as measured by the square root of the mean squared scattering angle, and a coefficient of "apparent absorption," which measures the transmitted fraction. In the range of total diffusion the change of transmission with thickness can be approximated by an exponential law.[35] This transmission law is independent of initial energy, atomic number, and film thickness. Our experimental data reveal that the relation between transmission and scattering angle holds not only for the range of "total diffusion" but also for relatively high transmissions or correspondingly small scattering angles.

[35] As shown by Bethe, Rose, and Smith[4] the correct treatment of the elementary diffusion equation leads to a decrease in transmission roughly inversely proportional to the film thickness rather than to an exponential law. This, however, should not change the general conclusion arrived at by Bothe.

2. The Dependence of Scattering Angle and Energy Loss on Z

In the following section we will outline qualitatively the main features of the observed experimental results for the dependence of the average scattering angle and the fractional average energy loss on the atomic number of the scatterer. Only such effects will be considered which in a single collision lead to appreciable scattering angles or energy loss. Small contributions due to characteristic losses will be neglected (see below).

A theoretical relation between the average scattering angle and the atomic number in a single inelastic collision with a free atom can be obtained using Bethe's approximate formula[7] for the average deflection angle θ_0 in collisions with electrons bound with energy I_0

$$\sin^2\theta_0\approx I_0/E, \tag{1}$$

where E is the initial energy of the scattered electron. We assume that the relation (1) holds also for the average scattering angle on atoms with a large spread in binding energies, if the average ionization potential is inserted in Eq. (1). The average ionization potential in turn is known to be proportional to the average excitation potential $\bar{I}$. This latter quantity, however, increases nearly linearly with Z for the lower atomic numbers.[36] Therefore, the square of the sine of the average inelastic scattering angle should increase approximately linearly with Z. Because the number of valence electrons represents a relatively small fraction of all electrons with which the primary can interact, this relation should also apply for atoms closely packed in solid matter.

The final average scattering angle after transmission through thin films depends on the mean scattering

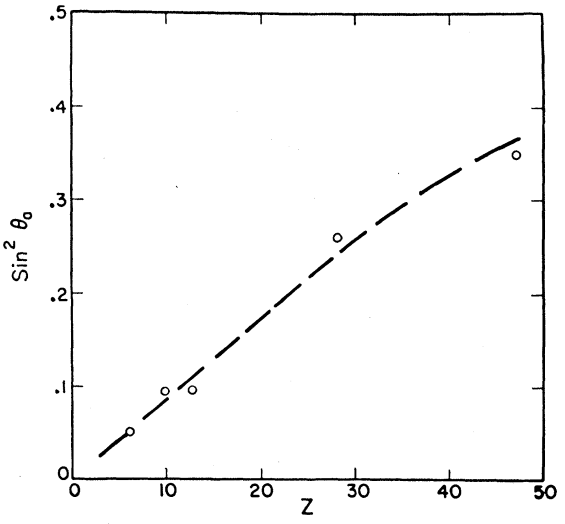

FIG. 14. Sine squared of the average scattering angle θ_a as a function of atomic number for $E_p=8$ kev and $D=300$ A. The target materials are C, Al_2O_3, Al, Ni, and Ag, respectively.

[36] F. Bloch, Z. Physik **81**, 363 (1933).

TABLE I. Comparison of experimentally and theoretically estimated number of inelastic collisions in thin films 300 A thick. $E_p=8$ kev.

1 Element, Z	2 $\bar{I}$ ev	3 $\Delta E_a/\bar{I}$	4 s
C, 6	76	9	9
Al, 13	150	7	6
Ni, 28	276	6	10
Ag, 47	418	4.5	5
Au, 79	680	3.7	5

angle for single collisions as well as on the scattering mean free path. In order to allow an estimate as to the Z dependence of the mean free path, $\sin^2\theta_a$ as measured on thin films about 300 A thick has been plotted as a function of Z in Fig. 14. The initial energy was $E_p=8$ kev. For the range of Z shown, $\sin^2\theta_a$ increases nearly linearly with Z. For larger Z, $\sin^2\theta_a$ increases less rapidly and finally levels off at a constant value of 0.5. This results from the fact that in high-Z materials even for a foil thickness as small as 300 A the electrons emerge in a state of total diffusion as manifested by the existence of a cosine distribution for which $\sin^2\theta_a=0.5$. Because of the fact that $\sin^2\theta_a$ measured on films of equal thickness but different Z varies nearly linearly with Z as would be expected for a single collision process, one can conclude that the number of collisions, or the mean free path for inelastic processes, does not depend strongly on Z.

In order to estimate roughly the number of strong inelastic collisions in films 300 A thick, we make use of the fact that per primary collision on the average an energy equal to the mean excitation potential $\bar{I}$ is transferred to the atomic electrons.[37] The number of such collisions can then be calculated from the average energy loss ΔE_a experienced by the transmitted electrons, divided by $\bar{I}$. For $\bar{I}$ experimental values obtained by Bakker and Segrè[38] were used. The results are presented in Table I, column 3. In agreement with the conclusion drawn from the observations on the squared average scattering angle, the number of collisions varies by only a factor 2.5 although the atomic number increases by a factor of 13. Because of the relatively low electron energies employed in our experiments, the listed values for the mean excitation potential actually need to be lowered for high-Z materials due to binding effects. Therefore, the values in column 3 tend to come out too small for high-Z materials, thus tending to further decrease the variation of the number of collisions with Z.

A comparison of these results with theoretical predictions of the mean free path for inelastic collisions is of interest. According to the Bohr-Bethe theory, the average number of inelastic collisions per unit path lengths can be calculated by[37]

$$s=\frac{2\pi e^4 N}{E}\sum_{n,l}\frac{Z_{n,l}}{I_{n,l}}\ln\frac{2E}{I_{n,l}}, \tag{2}$$

where N is the number of atoms per cm^3, E the energy of the scattered electron, $Z_{n,l}$ the number of electrons in the (n,l) shell, and $I_{n,l}$ the excitation energy, roughly equal to their binding energy. Using this formula and assuming that E remains essentially unchanged we find for the number of inelastic collisions in films 300 A thick the values listed in column 4 of Table I. For the outermost electrons an estimate for the excitation energy was taken as twice the work function, while for the inner shells the ionization potentials were determined from x-ray data. Reasonable agreement exists with the values calculated from the average energy loss ΔE_a and the experimental values of $\bar{I}$ (column 3).

It is seen that in Al, there occur on the average 6 to 7 collisions with individual atomic electrons leading to a total energy loss of about 1000 ev. In order to compare this with the energy loss due to possible collective interactions in Al, we may use the experimental results on the mean free path for these losses obtained by Blackstock, Ritchie, and Birkhoff.[39] These authors worked with electrons in the energy range from 20 to 100 kev. According to their results, the mean free path for the characteristic losses decreases about proportionally with energy. Extrapolating to lower energies, one finds that at 8 kev an electron suffers no more than 2 to 3 characteristic losses in an aluminum film 300 A thick. The principal characteristic loss in Al is 15 ev. Therefore, the energy dissipation associated with the discrete losses due to collective interaction is in the order of 50 ev, which can be neglected in comparison with the observed average loss of 1000 ev. The fraction due to characteristic losses in high Z material will be even smaller.

According to Fig. 8 the fractional average energy of electrons that have passed through thin films shows practically no dependence on Z when plotted as a function of E_p/E_c. This means that the average energy of electrons that have passed through films of equal E_c, or approximately equal mass per unit area, depends only on the initial energy E_p and not on the atomic number of the film material. This fact might be explained as follows: The thickness of films of equal mass per unit area varies inversely with Z, since the mass density of the elements increases roughly proportionally to Z. Because the mean free path for inelastic collisions does not vary appreciably with Z, the number of collisions in films of equal mass per unit area also varies inversely with Z. On the other hand, for sufficiently large energies, the energy loss per collisions is in the order of the average excitation potential $\bar{I}$, which

[37] N. Bohr, Kgl. Danske Videnskab. Selskab, Mat.-fys. Medd. **18**, No. 8 (1948).
[38] C. J. Bakker and E. Segrè, Phys. Rev. **81**, 489 (1941).
[39] A. W. Blackstock, R. H. Ritchie, and R. D. Birkhoff, Phys. Rev. **100**, 1078 (1955).

increases nearly linearly with Z.[36] Therefore, the average energy loss in films of equal mass density is practically independent of Z, as is indeed observed (Fig. 8).

Turning next to the Z dependence of the average scattering angle θ_a as a function of E_p/E_c (Fig. 10), it will be recalled that the square of the sine of the average scattering angle per collision, θ_0, is proportional to the individual average energy loss. Therefore, $\sin^2\theta_0$, or roughly θ_0^2, varies linearly with Z. Applying the well known additivity of mean squared fluctuations for independent events one can set $\theta_a^2 \approx s\theta_0^2$, where s refers to the number of collisions. Using the same reasoning as in the preceding paragraph, one might expect θ_a^2 and thus θ_a also to be essentially independent of Z. Of course, this argument would only be expected to hold if the scattering were entirely inelastic. As can be seen in Fig. 10, there is in fact a noticeable change of θ_a with Z, particularly for $Z \leq 30$. This can apparently be attributed to the effect of elastic scattering for the following reasons: The amount of elastic scattering increases with the effective nuclear charge. For the case of kilovolt electrons, however, the relative effect of screening by the more firmly bound electrons on the nuclear charge will be different for elements of low and high atomic number. Thus, for heavy elements, whose inner shells have binding energies in excess of several kev, the effective nuclear charge determining the elastic scattering remains approximately constant as Z increases while it grows with Z for the lighter elements. For the energy range under consideration, one should therefore expect a Z dependence only for the lower atomic number materials which is indeed observed experimentally as shown in Fig. 10.

The above considerations are, of course, only qualitative in nature. Nevertheless, they tend to confirm the conclusions arrived at by Sternglass in backscattering experiments, namely that at energies in the kev range, the scattering process is predominantly inelastic. The results furthermore indicate that even in this low-energy range the Bohr-Bethe theory may be applied to electron interaction processes in solids, as also concluded by Young[16] on the basis of range measurements down to 500 ev.

SUMMARY AND CONCLUSION

1. For electrons with energies between 1 and 10 kev the dependence of the transmitted fraction, average energy and scattering angle on initial energy, film thickness and material has been measured. The results can be represented as universal curves in terms of the critical energy E_c below which the emerging electrons are completely diffused.

2. In agreement with recent data by Holliday and Sternglass[32] for electron energies below 10 kev, the range-energy relation shows no significant dependence on Z when the range is measured in mass per unit area.

3. For sufficient film thickness, a direct relation between transmission and scattering angle exists. Except for high transmission, the relation between transmission and scattering angle is practically independent of the atomic number of the scattering material. This reveals the predominant dependence of the transmission process on scattering, even for these relatively low initial energies. For the process of "total diffusion" the observed relations were predicted by elementary diffusion theory.[3] The dependence of transmission on the atomic number Z is consistent with that observed for the backscattering coefficient from metals.[11]

4. The dependence of the average scattering angle and the average energy loss on the atomic number of the scatterer, confirms the conclusion drawn from backscattering measurements[11] that at energies below 10 kev the scattering process is predominantly inelastic. An estimate of the mean free path for inelastic collisions proves to be in good agreement with the predictions of the Bohr-Bethe theory.

The results confirm the need for an adequate theory of low-energy electron scattering by solids. In such a theory inelastic collisions must determine the elementary deflection process. The theory must account for the participation of the more firmly bound electrons in the scattering process and the fact that this participation varies with the energy of the penetrating electrons. The scattering process by itself should account for the transmission characteristic of the material, leaving the accompanying energy loss process as a second order correction.

ACKNOWLEDGMENTS

The author wishes to thank Dr. E. J. Sternglass for many discussions and for help in preparing the final form of the manuscript. The assistance of R. K. Matta throughout the course of this work, particularly in preparing the thin films, is acknowledged with gratitude.